Environmental Science & Technology

Article

High-throughput analysis of enzymatic hydrolysis of biodegradable polyesters by monitoring co-hydrolysis of a polyester-embedded fluorogenic probe

Michael Thomas Zumstein, Hans-Peter E. Kohler, Kristopher McNeill, and Michael Sander

Environ. Sci. Technol., **Just Accepted Manuscript** • DOI: 10.1021/acs.est.6b06060 • Publication Date (Web): 31 Jan 2017

ACS Publications

Environmental Science & Technology is published by the American Chemical Society. 1155 Sixteenth Street N.W., Washington, DC 20036

Manuscript

High-throughput analysis of enzymatic hydrolysis of biodegradable polyesters by monitoring co-hydrolysis of a polyester-embedded fluorogenic probe

Michael Thomas Zumstein[†], Hans-Peter E. Kohler[§], Kristopher McNeill[†], and Michael Sander[†,*]

[†] Institute of Biogeochemistry and Pollutant Dynamics, ETH Zurich, 8092 Zurich, Switzerland

[§] Environmental Biochemistry Group; Environmental Microbiology, Swiss Federal Institute of Aquatic Science and Technology (Eawag), 8600 Dübendorf, Switzerland

Submitted to *Environmental Science and Technology*

*To whom correspondence should be addressed.
E-mail: michael.sander@env.ethz.ch
Phone: +41-(0)44 6328314
Fax: +41 (0)44 633 1122

Number of pages: 25
Number of schemes: 1
Number of figures: 3
Number of tables: 1
Total word count: 7355 words (including 300 word equivalents for scheme 1, Table 1, and Figure 1 and 600 word equivalents for Figures 2 and 3).

Abstract

Biodegradable polyesters have the potential to replace non-degradable, persistent polymers in numerous applications and thereby alleviate plastic accumulation in the environment. Herein we present an analytical approach to study enzymatic hydrolysis of polyesters, the key step in their overall biodegradation process. The approach is based on embedding fluorescein dilaurate (FDL), a fluorogenic ester substrate, into the polyester matrix and on monitoring the enzymatic co-hydrolysis of FDL to fluorescein during enzymatic hydrolysis of the polyester. We validated the approach against established techniques using FDL-containing poly(butylene adipate) films and *Fusarium solani* cutinase (FsC). Implemented on a microplate reader platform, the FDL-based approach enabled sensitive and high-throughput analysis of the enzymatic hydrolysis of eight aliphatic polyesters by two fungal esterases (FsC and *Rhizopus oryzae* lipase) at different temperatures. While hydrolysis rates for both enzymes increased with decreasing differences between the polyester melting temperatures and the experimental temperatures, this trend was more pronounced for the lipase than the cutinase. These trends in rates could be ascribed to a combination of temperature-dependent polyester chain flexibility and accessibility of the enzyme active site. The work highlights the capability of the FDL-based approach to be utilized in both screening and mechanistic studies of enzymatic polyester hydrolysis.

Introduction

The accumulation of persistent plastic material in aquatic and terrestrial systems has become a major environmental concern.[1-3] One strategy to overcome this problem is to replace non-degradable with biodegradable polymers, particularly when used in

short-term applications, including packaging and agriculture.[4-8] Among the commercially important biodegradable polymers are polyesters that contain ester bonds susceptible to hydrolytic cleavage.[7-9] Ester bond hydrolysis is considered the rate-limiting step in overall polyester degradation in natural and engineered systems[9,10] and results in the release of oligomers and monomers that can be utilized by microorganisms.

Pioneering work showed that extracellular microbial hydrolases are active on ester bonds in synthetic polyesters.[11] A number of analytical approaches have since been developed to screen for enzymes and organisms capable of hydrolyzing polyesters and to study enzymatic polyester hydrolysis on a mechanistic level. The screening approaches include clearing-zone assays,[12] liquid turbidimetric assays,[13] and assays that monitor the release of soluble hydrolysis products into solution by total organic carbon (TOC)[11] or liquid chromatography-mass spectrometry measurements.[14-16] These approaches enabled the identification of various hydrolases (e.g. cutinases, lipases, and esterases) that are active on synthetic polyesters, including poly(lactic acid), poly(caprolactone), poly(butylene succinate), poly(butylene adipate-co-terephthalate), and poly(ethylene terephthalate).[12,17-21] An analytical approach commonly used in mechanistic studies is pH-stat titration in which the number of hydrolyzed ester bonds are quantified by automated titration of released protons with base.[22,23] Recent work from our group demonstrated that *in situ* quartz crystal microbalance with dissipation monitoring (QCM-D) measurements are an additional analytical tool that allows to directly monitor the mass loss of spin-coated polyester thin films during enzymatic hydrolysis.[24,25] While successfully applied in numerous studies, the above approaches have in common that they meet one or more of the following analytical challenges: (i) only a small number of hydrolysis experiments

can be run in parallel, (ii) the hydrolysis dynamics cannot be monitored in real time, (iii) samples need to be (manually) withdrawn from hydrolysis experiments for ex situ analysis, and (iv) specialized and/or expensive laboratory equipment is required.

One promising conceptual approach to overcome these challenges is to follow polyester hydrolysis by monitoring the co-hydrolysis of ester-based fluorogenic probes embedded into the polyester. Fluorogenic probes are non-fluorescent and only become fluorescent upon hydrolysis of the intramolecular ester bond(s) of the probe.[26] This approach could be implemented on a fluorescence microplate platform for high sample throughput, similar to the use of dissolved fluorogenic probes in functional screening assays to identify organisms and enzymes that hydrolyze ester bonds (i.e. carboxylic-ester hydrolases, hereafter referred to as esterases).[27,28] While dissolved fluorogenic probes may not reveal the capability of enzymes to depolymerize insoluble polyesters,[29] fluorogenic probes that are embedded in the polyester would be hydrolyzed only in the presence of esterases that hydrolytically remove the polyester matrix surrounding the embedded probe. Because of higher sensitivity of fluorescence than absorbance measurements, an assay based on the conversion of an embedded fluorogenic probe is expected to have lower detection limits than assays that rely on embedded chromophoric probes.[30] Furthermore, given that chromophoric probes also absorb light in their polymer-embedded form, the release of such probes cannot be readily followed in *in situ* microplate experiments.[30] In contrast, embedded fluorogenic probes are non-fluorescent and thus do not interfere with fluorescence detection of hydrolyzed probes.

The goal of this work was to develop and validate an enzymatic polyester hydrolysis approach that is based on monitoring fluorescence originating from the co-hydrolysis of a polyester-embedded fluorogenic probe. We chose fluorescein dilaurate

(FDL) as probe (**Scheme 1**) because we expected that the laurate groups effectively anchor the probe in the polyester matrix and thereby minimize probe leaching from the polyester. Furthermore, the hydrolysis product fluorescein is highly water-soluble and readily detectable by fluorescence measurements. In a first step, we compared the dynamics of fluorescein release from embedded FDL during the enzymatic hydrolysis of poly(butylene adipate) films to the hydrolysis dynamics of the same films simultaneously detected using pH-stat titration and QCM-D measurements. In a second step, we implemented the method on a microplate platform and studied the hydrolysis of a series of eight aliphatic polyesters by two esterases from soil fungi, a cutinase from *Fusarium solani* (FsC) and a lipase from *Rhizopus oryzae* (RoL), at four different temperatures. The set of polyesters was chosen because they are of commercial importance, cover a range of physicochemical properties, and include polyesters synthesized from bio-based monomers.[31] Furthermore, the enzymatic hydrolysis of a subset of these polyesters has previously been investigated,[22,23] thereby providing a reference for the results obtained with the new FDL-based approach.

[insert Scheme 1 here]

Scheme 1. a. Enzymatic hydrolysis of the fluorogenic probe fluorescein dilaurate (FDL) (R = $-(CH_2)_{10}CH_3$) into fluorescein (F) with fluorescein monolaurate as an intermediate hydrolysis product. **b. – e.** Schematic of the enzymatic hydrolysis of a polyester film showing the enzymatic co-hydrolysis of polyester-embedded FDL to F, which is subsequently released into solution and detected by fluorescence measurements.

Materials and Methods

Chemicals and Solutions. Fluorescein dilaurate (FDL, product number: 46943), fluorescein (46955), dioctyl phthalate (D201154), dibutyl adipate (309494), and *para*-nitrophenol butyrate (N9576) were obtained from Sigma-Aldrich. All chemicals used were of high purity (at least > 95%) and used as received. A list of all other chemicals

used are provided in the Supporting Information (SI). All solutions were prepared in Milli-Q water (resistivity = 18.2 MΩ cm; Barnstead NANOpure Diamond) and contained 10 mM KCl as background electrolyte.

Enzymes. Cutinase from *Fusarium solani* (FsC, molecular weight (M_w): 20.8 kDa, isoelectric point (pI): 8.4, both calculated from the sequence entry 1AGY[32] in the RCSB Protein Data Base (PDB) using the pI/MW compute tool from expasy[33]) was obtained from ChiralVision (product number Novozym 51032) as a solution (nominal concentration, determined by absorbance measurements at 280 nm and a molar extinction coefficient of 13610 M^{-1} cm^{-1}:[34] 4.24 ± 0.16 mM (mean ± standard deviation of triplicate measurements)). Lipase from *Rhizopus oryzae* (RoL, M_w: 29.6 kDa, pI: 8.1, PDB entry 1TIC[35]) was obtained from Sigma Aldrich as a powder (product number 80612). We prepared enzyme stock solutions of comparable catalytic activities (see below) in a pH-buffered solution (3 mM phosphate, pH 6.0) at 4.1 mg FsC/mL and 100 mg RoL/mL. The stocks solutions were aliquoted and stored at -20 °C until use.

We determined the hydrolytic activities of FsC and RoL using the soluble model substrate *para*-nitrophenol butyrate.[36] Briefly, 20 µL of an enzyme solution (concentrations of 1.4 µg FsC/mL and 3.3 µg RoL/mL) and a pH 6 buffered solution (180 µL, 50 mM 2-(*N*-morpholino)ethanesulfonic acid (MES)) containing *para*-nitrophenol butyrate (final concentration in the well: 5 mM) were added to wells of a 96-well plate (product number: 269620, Nunc). The formation of the hydrolysis product *para*-nitrophenol was subsequently monitored by absorbance measurements at 405 nm at 30 °C in a temperature-controlled plate reader (Synergy HT, BioTek GmbH). The absorbance values were converted to *para*-nitrophenol concentrations

using a *para*-nitrophenol calibration curve constructed from standards run on the same plate.

We additionally determined the hydrolytic activities of FsC and RoL on an emulsified substrate, dibutyl adipate (DBA), using a pH-stat titration assay adapted from Marten and co-workers.[22] In brief, DBA (0.5 mL) and an emulsifier (9.5 mL, 0.32 g/mL glycerol, 3 mg/mL gum arabicum, 10 mM KCl) were equilibrated in a thermo-jacketed beaker at pH 6 and 30 °C. After addition of enzyme stock solution (10 µL), the acid generated by ester hydrolysis was automatically titrated with KOH (10 mM) to maintain a constant solution pH (Titrando 907, Metrohm). The hydrolytic activity of the enzyme was calculated from the number of protons titrated within the first 10 minutes of esterase addition.

Polyesters. **Table 1** shows the generalized chemical structure of the polyesters studied and their key physicochemical properties. The polyesters were kindly provided by BASF SE.

Table 1. Generalized structural formula and key physicochemical properties of the studied aliphatic polyesters. T_m, M_n, M_w, and n refer to the melting temperature, the number average molecular weight, the weight average molecular weight, and the number of carbon atoms in the diacid component in the polyester, respectively. For PBC_6, these properties were previously published.[24] M_n and M_w of PBC_{18} were not measurable (n.m.).

[insert Table 1 here]

pH-stat titration experiments. PBC_6 films with approximate thicknesses of 30 µm were produced by casting chloroform solutions containing PBC_6 (0.5 % (w/w)) and FDL (0.0005 % (w/w)) into glass petri dishes, followed by solvent evaporation. The films were brought in contact with liquid nitrogen for 3 min prior to removal from the petri dish. Circular polyester film pieces (diameter: 2.25 cm) were punched out of the cast film using an arch punch. The subsequent pH-stat titration assay was

adapted from the literature.[22] In brief, the film pieces were transferred into a thermo-jacketed beaker (30 °C) containing 15 mL of a KCl solution (10 mM). The solution pH was set to pH 6 and subsequently kept constant by automated pH-stat titration using a Titrando 907 (Metrohm) delivering a KOH solution (10 mM). The system was allowed to equilibrate for one hour prior to the addition of the FsC stock solution (64 µL; final concentration of 17.6 µg FsC/mL). The number of hydrolyzed ester bonds in PBC_6 was directly quantified by the number of hydroxide ions added to maintain a constant solution pH. Throughout the hydrolysis, 0.5 mL solution aliquots were withdrawn and analyzed for the released amounts of fluorescein and total organic carbon (TOC). Solution fluorescence was measured after 10-fold dilution in milli-Q water on black polypropylene 96-well plates using a fluorescence microplate reader (SynergyHT, BioTek, excitation at 485±20 nm and emission at 528±20 nm) and converted to fluorescein concentrations employing a calibration curve constructed from fluorescein standards (1 to 400 nM) run on the same microplate. For TOC measurements, sampled aliquots (400 µL) were diluted in Milli-Q water (7.6 mL) and filtered (0.22 µm pore size syringe filters, PP+GF filter, BGB) into a test tube (Shimadzu). The signal of the TOC analyzer (TOC-L, Shimadzu) was converted to a TOC concentration employing a standard calibration curve (0 to 20 mg C/L) prepared from a TOC standard (Fluka).

QCM-D measurements. We adapted the QCM-D-based approach described in Zumstein et al.[24] In brief, small volumes (40 µL) of a chloroform solution with PBC_6 (final concentration: 0.5% w/w) and FDL (0.005% w/w) were transferred onto QCM-D sensors (QSX 301, Q-Sense) fixed horizontally in a spin coater (model: WS-650MZ-23NPP, Laurell Technologies). The sensor was then spun at 4000 rpm for 1 minute (acceleration: 1500 rpm/s).

The PBC_6-coated sensors were pre-equilibrated to the experimental solutions (i.e., pH 6, 3 mM sodium phosphate, filter sterilized with 0.2 μm cellulose acetate filters, Target)) for 14 h at 25 °C before being individually mounted into one of four flow cells of a QCM-D E4 unit (Q-Sense). The QCM-D was used to continuously monitor changes in the masses and the viscoelastic properties of the PBC_6 films during hydrolysis by detecting the associated shifts in the resonance frequencies, Δf_i (Hz), and the energy dissipation values, ΔD_i, at the fundamental (i= 1) and several oscillation overtones (odd numbers between i= 3 and 15) of a piezo-quartz crystal embedded into each sensor. The Sauerbrey equation (Eq. 1) was used to calculate changes in the mass of the adsorbed film, Δm (ng/cm^2):

$$\Delta m = C * -\frac{\Delta f_i}{i} \qquad \textbf{Eq. 1}$$

where C (17.7 $ng/(cm^2 \bullet Hz)$) is the sensor-specific mass sensitivity constant. We used the fifth overtone (i= 5) for calculations and plotting.

During the entire hydrolysis experiment, the outflow from each QCM-D flow cell was collected in fractions in which the fluorescein concentration was determined as detailed above. At the onset of each individual hydrolysis experiment, the PBC_6 film was equilibrated to the experimental solution and temperature conditions by running a degassed, esterase-free solution (3 mM phosphate, pH 6) through the flow cell over the sensor surface at a constant volumetric flow rate (20 μL/min). Upon attainment of stable Δf_i and ΔD_i readings, an enzyme-containing solution (4.4 μg FsC/mL) of the same pH and temperature was delivered to the flow cell at the same flow rate. The ensuing PBC_6 hydrolysis was monitored until Δf_i and ΔD_i re-attained stable values. The sensor was then removed from the flow cell, dipped into Milli-Q water and dried under a stream of N_2. We independently determined the mass fraction of each coated PBC_6 thin film that was hydrolytically removed from the sensor by

resonance frequency measurements of the dried sensor before and after spin coating, as well as after the hydrolysis experiment. The QCM-D system and sensors were cleaned in between measurements as detailed in the SI.

Microplate assay. Polyester films were cast onto the bottom of the wells of a black polypropylene 96 well microplates (655209, Greiner Bio-One) from a chloroform solution containing 0.5 % (w/w) polyester and 0.0005 % (w/w) FDL. Coating involved the transfer of 40 μL of the chloroform solution into each well, followed by shaking the plate on an orbital shaker (160 rpm) in a fume hood for 24 h to ensure complete chloroform evaporation.

The polyester films were equilibrated to a pH 6-buffered solution (volume: 242.5 μL; 150 mM MES) for one hour during which fluorescence was monitored every 10 min in a temperature-controlled plate reader (Synergy HT, BioTek or Infinite 200PRO, Tecan). Before each reading, the plate was shaken for 3 s. Enzyme stock solution (7.5 μL) was then added and the fluorescence was continuously recorded every 10 min throughout the polyester hydrolysis. The amount of fluorescein released from the polyester films was calculated using a fluorescein calibration curve (concentrations of 0.01 to 3 μM) run on each plate.

Results and Discussion

Method validation. We compared the fluorescein release dynamics during the enzymatic hydrolysis of PBC_6 films that contained FDL to the hydrolysis dynamics simultaneously monitored by three established techniques: pH-stat titration, TOC analysis, and QCM-D measurements.

Comparison to pH-stat titration and TOC release measurements. We used PBC_6 films that contained approximately 0.1% (w/w) FDL. **Figure 1a** shows the

cumulative number of hydrolyzed ester bonds and the cumulative amounts of TOC and fluorescein that were released into solution during the hydrolysis of a representative PBC_6 film by *Fusarium solani* cutinase (FsC). Prior to cutinase addition at time < 0 min, the solution pH was stable at pH 6 without base addition. Consistently, neither TOC nor fluorescein was released into solution. These findings implied that leaching and non-enzymatic hydrolysis of FDL were negligible. These two commonly-recognized challenges of fluorogenic ester probes[27,37] therefore did not affect our measurements.

Addition of cutinase at t = 0 min triggered enzymatic hydrolysis of ester bonds in the PBC_6 film and co-hydrolysis of embedded FDL, as evidenced from the onset of base titration and increasing solution TOC and fluorescein concentrations. The sigmoidal titration and release curves imply that hydrolysis rates first increased, reached maxima, and subsequently decreased. While the PBC_6 film had visually disappeared approximately 80 min after cutinase addition, hydrolysis continued up to about 200 minutes when all curves plateaued. At this time, complete PBC_6 hydrolysis was attained, given that the cumulative number of hydrolyzed ester bonds, determined from base titration, corresponded well to the calculated number of ester bonds in the originally added PBC_6 film (98 ± 16 % (mean ± deviations of duplicates) of calculated values). Furthermore, the cumulative amounts of released TOC and fluorescein corresponded to 89 ± 7 % of the calculated carbon added as PBC_6 and 103 ± 5 % of the initially embedded FDL.

The good agreement between the curves describing ester hydrolysis and TOC release implies that the hydrolysis products in solution were mostly monomeric, consistent with previous reports of complete PBC_6 hydrolysis by cutinases and cutinase-like hydrolases.[9,18] The onset of fluorescein-release showed a time delay

283 relative to base addition and TOC release. This delay may have resulted from a non-
284 uniform distribution of FDL in the PBC_6 film (with higher concentrations in the
285 center of the film) and would result in a slight underestimation of the initial rate of
286 polyester hydrolysis. However, the observed delay supports that no FDL had diffused
287 to the polymer surface where it would undergo more rapid enzymatic hydrolysis.
288 More importantly, fluorescein was rapidly released when the film started to visually
289 disintegrate and FDL and PBC_6 hydrolysis were completed at the same time.

290 Control experiments using FDL-free PBC_6 films (**Figure S1a**) showed rates and
291 extents of ester bond hydrolysis and TOC release that were indistinguishable from
292 those measured for FDL-containing PBC_6 films. The small amounts of FDL in the
293 PBC_6 matrix therefore did not affect enzymatic hydrolysis of the films.

294 [insert Figure 1 here]

295 **Figure 1**. Hydrolysis of poly(butylene adipate) (PBC_6) films by *Fusarium solani*
296 cutinase (FsC) (added at time t= 0 min) at 30 °C and pH 6. **a.** Hydrolysis of a solvent-
297 cast PBC_6 film containing 0.1% (w/w) fluorescein dilaurate (FDL) as assessed by
298 automated pH-stat titration in a thermo-jacketed beaker. Cumulative ester bonds
299 hydrolyzed (black line, left ordinate; quantified from the amount of base titrated) and
300 cumulative amounts of total organic carbon (TOC, blue open circles, right ordinate)
301 and fluorescein (green-filled circles; right ordinate) released into solution over time.
302 **b.** Hydrolysis of a spin-coated PBC_6 thin film containing 1% (w/w) FDL as assessed
303 by quartz crystal microbalance with dissipation monitoring (QCM-D) measurements
304 and quantification of fluorescein concentrations in the effluent of the QCM-D flow
305 cell. Cumulative mass released from the sensor surface (black line; left ordinate) and
306 cumulative amount of fluorescein released (green-filled circles; right ordinate) over
307 time.

308 *Comparison to QCM-D measurements.* The spin-coated PBC_6 films with
309 approximately 1% (w/w) of embedded FDL had an average mass of 6.5 ± 0.3 μg
310 (mean ± deviations of duplicates, as determined by QCM-D measurements of the
311 sensors in air) and thicknesses of approximately 80 nm.[24] Control films without FDL
312 had the same masses (6.490 ± 0.003 μg) and thicknesses, demonstrating that the
313 presence of FDL did not noticeably affect the spin coating.

Figure 1b shows the cumulative released mass and the cumulative amount of released fluorescein during the hydrolysis of a representative PBC_6 film by the cutinase. During equilibration of the PBC_6 film at time $t < 0$ min to an enzyme-free solution (pH 6, 30 °C), the adsorbed mass was stable and no fluorescein was released, demonstrating that non-enzymatic PBC_6 and FDL hydrolyses were negligible. PBC_6 hydrolysis started immediately after switching to the cutinase-containing solution at time = 0 min, as evidenced from the onset of mass loss and the simultaneous release of fluorescein into solution. The mass and fluorescence release curves leveled off approximately two hours after cutinase addition and plateaued at the end of the experiment. Following sensor removal from the flow cells and drying, measurements of the resonance frequencies of the sensors showed that the final mass corresponded to only 7 ± 3 % (mean ± deviations of duplicates) of the initially spin-coated PBC_6 mass. Because the final mass included the mass of cutinase molecules adsorbed to the bare sensor surface that became exposed upon PBC_6 film hydrolysis,[24] we conclude that the cutinase removed most, if not all, of the spin-coated PBC_6 mass. We note that the total amount of fluorescein released at the end of the experiment was 130 ± 11% (mean ± deviations of duplicates) of the calculated embedded amount of FDL, suggesting that the PBC_6 films had a slightly higher FDL mass fraction (1.3%) than in the chloroform solution used for spin coating (1%). Control experiments showed that this FDL concentration did not affect PBC_6 hydrolysis by the cutinase (**Figure S1b**). The overall good agreement between the mass loss and fluorescence release curves validate the use of the FDL-based approach to monitor polyester hydrolysis.

Implementation on microplate platform. PBC_6 films that contained FDL (0.1% (w/w)) were solvent-cast onto the flat bottom of microplate wells. **Figure 2a,b** show the cumulative amounts of fluorescein released during the hydrolysis of these films by

339 either *Fusarium solani* cutinase (FsC) or *Rhizopus oryzae* lipase (RoL) at 30 °C and
340 pH 6. The error bars represent the deviations of triplicate experiments, demonstrating
341 that the analyses were highly reproducible. For clarity of the presentation, we later
342 show fluorescein release curves from single representative experiments.

343 Prior to enzyme addition at $t < 0$ min, no fluorescein was detected in the
344 microplate wells containing PBC_6 films with embedded FDL, again demonstrating
345 that non-enzymatic hydrolysis of PBC_6 and FDL were negligible. The addition of
346 cutinase or lipase at time = 0 h resulted in polyester hydrolysis, as evidenced from
347 increasing fluorescein concentrations. Approximately 1.5 h and 3.5 h after addition of
348 cutinase and lipase, respectively, the cumulative amounts of released fluorescein
349 reached a plateau at 0.35 nmol. This amount was in good agreement with the
350 calculated amount of FDL embedded into the PBC_6 films, strongly suggesting that
351 both enzymes extensively hydrolyzed the PBC_6 films.

352 A set of control experiments served to rule out potential measurement artifacts.
353 First, we measured the fluorescein release from non-embedded FDL (i.e., FDL
354 solvent-cast into microplate wells from a chloroform solution without PBC_6). For both
355 FsC and RoL, fluorescein release rates were much higher for non-embedded than for
356 FDL that was embedded in PBC_6 films, showing that the hydrolysis of surrounding
357 PBC_6 was controlling the release of fluorescein (**Figure S2**). Second, polyester films
358 containing FDL showed no signs of both probe leaching and of non-enzymatic
359 hydrolysis over an 8-hour incubation in enzyme-free solutions (**Figure S3**).
360 Conversely, fluorescein diacetate (FDA), a structurally similar but smaller fluorogenic
361 probe, both leached out of polyester films and underwent non-enzymatic hydrolysis.
362 These findings corroborate that the laurate groups in FDL were critical to anchor the
363 probe in the polyester matrix. These control experiments confirmed that fluorescein

release dynamics from polyester-embedded FDL truly reflect the dynamics of enzymatic polyester hydrolysis.

Comparing the fluorescein release dynamics from PBC_6 films during hydrolysis by the two enzymes resulted in two major findings. First, FsC was more active on PBC_6 than RoL: while the enzymes showed comparable initial hydrolysis rates of PBC_6, an approximately 24-fold higher concentration of RoL than FsC was used. The higher activity of FsC on PBC_6 was also more pronounced than on the two non-polymeric substrates *para*-nitrophenol butyrate and dibutyl adipate (6- and 14-fold higher, respectively) (**Table S1**). Second, following comparable initial fluorescein release rates, the hydrolysis dynamics of the PBC_6 films by the two enzymes markedly diverged (**Figures 2a,b**): while the use of FsC resulted in a sigmoidal fluorescein release curve, the rate of RoL-mediated fluorescein release slowed down when approximately 50 to 60% of the fluorescein was released. The phase of slower fluorescein release may have reflected that hydrolysis of PBC_6 films by RoL progressed through extensively hydrated film intermediates that slowed down RoL-mediated hydrolysis. The formation of such intermediate states was recently demonstrated by QCM-D.[38] By comparison, FsC-mediated hydrolysis either did not progress through such water-rich film intermediates (e.g., due to more extensive lateral than depth erosion on the polyester surface by FsC as compared to RoL) or was less affected by film hydration. The latter explanation is supported by the fact that lipases require apolar surfaces to attain full activity (which would be impaired in well hydrated films) whereas cutinases do not require such surface activation.[39]

[insert Figure 2 here]

Figure 2. Enzymatic hydrolysis of aliphatic polyesters PBC_n composed of 1,4-butanediol (B) and aliphatic dicarboxylic acid components of variable length (C_n) (as

detailed in Table 1). All experiments were performed at pH 6 and 30 °C in a temperature-controlled microplate reader. Error bars represent standard deviations of triplicate measurements. **a.** - **d.** Cumulative amounts of fluorescein released during the hydrolysis of polyesters (PBC_n) containing embedded fluorescein dilaurate by *Fusarium solani* cutinase (FsC) and *Rhizopus oryzae* lipase (RoL). The error bars in panels a,b,e an f represent standard deviations of triplicate measurements. **e.** and **f.** Fluorescein release rates (estimated from the time required for the release of 0.2 nmol fluorescein, see dashed lines and formula in panels a and b) from PBC_n during hydrolysis by FsC and by RoL plotted versus the number of carbon atoms in the diacid component, n, and the melting temperature, T_m, of the polyesters.

Application of microplate platform. We studied the hydrolysis of eight aliphatic polyesters that all contained 1,4-butanediol but differed in the number of carbon atoms in the dicarboxylic acid building block (i.e., PBC_n; **Table 1**). Previously, authors who studied the hydrolysis of a subset of these polyesters reported decreasing enzymatic hydrolysis rates with increasing melting temperatures, T_m, of the tested polyesters.[22,23,40,41] This trend was ascribed to a decrease in the flexibility of polyester chains —and hence a decrease in the propensity of ester bonds to enter the active sites of esterases— with increasing T_m. The results of the previous studies served as a reference for the results obtained with the FDL-based approach. At the same time, the capability of the microplate platform for high sample throughput allowed us to extend the experimental matrix beyond those of previous studies, including a larger set of polyesters, a comparison of two esterases (FsC and RoL), and four experimental temperatures from 15 to 40 °C.

Effect of polyester structure on enzymatic hydrolysis. **Figures 2c,d** show representative fluorescein release curves during the hydrolysis of the tested aliphatic polyesters by FsC and RoL at pH 6 and 30 °C. While all polyesters were hydrolyzed by FsC within ten hours, PBC_4 and PBC_{18} —the polyesters with the shortest and longest dicarboxylic acid components, respectively— were not hydrolyzed by RoL. As discussed above for PBC_6, the fluorescein release dynamics differed between the two enzymes for all polyesters with n between 6 and 12: while FsC-mediated

hydrolysis resulted in sigmoidal fluorescein release curves, RoL-mediated hydrolysis resulted in bi-phasic fluorescein release curves.

We compared the hydrolysis rates, which we calculated from the time required until 0.2 nmol of fluorescein were released (see **Figures 2a,b** for examples), of the different polyester-enzyme systems. For both enzymes, hydrolysis rates were higher for PBC_6 to PBC_{10} than for PBC_4, PBC_{12}, PBC_{13}, and PBC_{18} (with no hydrolysis for RoL on PBC_4 and PBC_{18}) (**Figures 2e,f**; left panels). When re-plotted against T_m (**Figures 2e,f**; right panels), the hydrolysis rates decreased with increasing T_m, consistent with the trend reported previously and the polyester chain flexibility hypothesis.[22,23,40,41] The good agreement of our results with previous studies supports the use of the FDL-based microplate platform for mechanistic studies of enzymatic polyester hydrolysis.

The inverse relationship between hydrolysis rate and T_m was more strict for RoL than for FsC: while rates obtained with RoL continuously decreased with increasing T_m, this was not the case for FsC-mediated polyester hydrolysis. First, the hydrolysis rates of PBC_{10} and PBC_{12} were significantly higher than those of PBC_6 and PBC_{13}, respectively, despite the higher T_m of PBC_{10} and PBC_{12} than of PBC_6 and PBC_{13}, respectively. Second, despite its higher T_m, PBC_4 was hydrolyzed faster than PBC_{18}. The differences in the rates of polyester hydrolysis by RoL and FsC suggests that enzyme-specific factors controlled hydrolysis in addition to polyester-chain flexibility, as discussed in more detail below.

Effect of experimental temperature on enzymatic hydrolysis. Curves of fluorescein release during the hydrolysis of all polyesters at four $T_{experiment}$ (15, 20, 30, and 40 °C) by both enzymes are provided in **Figure S4**. For both enzymes, the rates of hydrolysis of all polyesters increased with increasing $T_{experiment}$ with the exception

of PBC_4 and PBC_{18} by RoL, for which no hydrolysis was detected even at 40 °C (**Figures 3a,b**). No detectable PBC_4 hydrolysis at 40 °C was in agreement with an earlier study that reported no lipase-mediated hydrolysis of PBC_4 at 50 °C.[22] We note that studies reporting PBC_4 hydrolysis by lipases were either conducted at higher temperatures (e.g., 70 °C) or were performed with non-crystalline PBC_4 nanoparticles.[42,23]

[insert Figure 3 here]

Figure 3. Fluorescein release rates during the hydrolysis of aliphatic polyesters (PBC_n) containing fluorescein dilaurate (FDL) by *Fusarium solani* cutinase (FsC; **a.** and **c.**) and *Rhizopus oryzae* lipase (RoL; **b.** and **d.**) at different experimental temperatures, $T_{experiment}$. The rates are plotted against the melting temperature (T_m) of the polyesters (panels a and b) and against the difference between T_m and $T_{experiment}$ (T_m-$T_{experiment}$; panels c and d). Error bars represent standard deviations of triplicate measurements. The data collected at 30 °C is re-plotted from Figures 2. All experiments were performed at pH 6 in a temperature-controlled microplate reader.

The rates of polyester hydrolysis at 15, 20 and 40 °C by both enzymes showed dependencies on the length of the dicarboxylic acid units that were similar to the dependency described above for 30 °C (**Figure S5**). More interestingly from a mechanistic perspective, the hydrolysis rates at all $T_{experiment}$ decreased with increasing T_m for both FsC and RoL (**Figure 3a,b**). This trend became much more distinct when re-plotting the rates versus the differences between T_m of the polyester and the experimental temperature, T_m-$T_{experiment}$ (**Figure 3c**,**d**). For RoL, the inverse relationship was particularly pronounced and revealed a threshold of T_m-$T_{experiment}$ = 45 °C, above which no hydrolysis by RoL was detected. By comparison, the inverse relationship between hydrolysis rate and T_m-$T_{experiment}$ was less pronounced for FsC. Furthermore, FsC hydrolyzed PBC_4 at all four temperatures despite the high corresponding T_m-$T_{experiment}$ values.

Mechanistic interpretation of differences in polyester hydrolysis by FsC and RoL. The tight inverse relationship between hydrolysis rate and T_m-$T_{experiment}$ for RoL is consistent with the polyester chain flexibility hypothesis:[22] as T_m-$T_{experiment}$ decreases, the chain flexibility and therefore the chance of ester groups in the polyester to reach the active site of RoL increased. In support of this explanation, we showed that hydrolysis rates of PBC_4 films by RoL increased markedly with increasing concentrations of the plasticizer dioctyl phthalate (**Figure S6**). At a plasticizer concentration of ~10 % (w/w), approximately 15% of the embedded fluorescein was released during a 10 h incubation. A similar approach was previously used to enhance enzymatic hydrolysis of poly(ethylene terephthalate).[43]

As compared to RoL, the less pronounced relationship between hydrolysis rate and T_m-$T_{experiment}$ for FsC and the comparatively high hydrolysis rates of PBC_4 by FsC strongly suggests that other factors in addition to polyester chain flexibility affected FsC-mediated hydrolysis. The comparatively low rates of PBC_{13} and PBC_{18} hydrolysis by FsC (**Figure 3a**) may have resulted from a combination of a low density of ester bonds on the polyester surface and a low solubility of the long chain dicarboxylic acids formed during hydrolysis.

A stronger dependence of the hydrolysis rate on the flexibility of polyester chains for RoL than for FsC can be rationalized by visualizing the active sites of these enzymes in their three dimensional structures. While the active site of RoL is located in a relatively deep pocket, the active site of FsC is more exposed on the enzyme surface (**Figure S7**). As a consequence, the formation of the enzyme-substrate complex is expected to require a higher polyester chain flexibility for RoL than FsC. This explanation is supported by a previous study that ascribed the hydrolytic activity

498 of a *Themobifida fusca* hydrolase on polyesters with high T_m to the surface-exposed
499 active site of the enzyme.[9]

500 The pronounced effect of active site accessibility on polyester hydrolysis rates
501 identified here likely applies more generally to lipases and cutinases. The active sites
502 of most lipases are covered by lid-like polypeptide chains. In a process called
503 'interfacial activation', these lids are lifted from the active site upon contact of the
504 lipases with apolar surfaces, thereby enhancing hydrolytic activities.[44,40] Such lid-like
505 structures are absent in cutinases and, as a consequence, cutinases usually have a
506 broader substrate spectrum than lipases[39,45] and presumably higher activities on
507 polyesters with high T_m. Indeed, most hydrolases that were shown to be active on
508 poly(ethylene terephthalate) (T_m > 200 °C) are classified as cutinases.[18-20,46] The
509 effect of active site accessibility on polyester hydrolysis can also be used in enzyme
510 engineering: enlarging the active site of FsC resulted in increased hydrolytic activity
511 on PET fibers.[47,48]

512 ***Implications***. In this work we developed and validated a sensitive approach to
513 study enzymatic polyester hydrolysis at high sample throughput. This approach is
514 based on the co-hydrolysis of a fluorogenic ester probe embedded in the polyester
515 matrix. We anticipate that this approach will become readily adopted in numerous
516 laboratories and will facilitate future work on various aspects of enzymatic polyester
517 hydrolysis. These include (i) screening studies aiming at identifying esterases and/or
518 microorganisms that are hydrolytically active on specific polyesters (e.g., to be used
519 in polyester recycling[49,50]) and, for identified esterases, determining hydrolyzability of
520 different biodegradable polyesters, including also aliphatic-aromatic co-polyesters,
521 (ii) mechanistic studies of enzymatic polyester hydrolysis as a function of polyester
522 chemical structure, enzyme properties, and hydrolysis conditions (e.g., temperature

and solution pH), and (iii) systematic assessments of the effects of polyester additives and/or polyester aging (e.g., photochemical alteration) on enzymatic hydrolysis. Given that enzymatic hydrolysis is the key step in polyester biodegradation in natural systems, the FDL-based assay will help to assess the potential of biodegradable polyesters to replace non-degradable polymers, thereby alleviating the problem of plastic accumulation in the environment.

Associated content

Supporting Information. Additional information and data on chemicals, and on QCM-D, pH-stat titration, and microplate reader experiments. This material is available free of charge via the Internet at http://pubs.acs.org.

Author information.

Corresponding author: * Email: michael.sander@env.ethz.ch

Notes

The authors declare no competing financial interest.

Acknowledgements.

We thank Prof. David Norris and Jan Winkler for access to the spin coater, and Prof. Shana Sturla and Céline Stäuble for access to a microplate reader. The authors thank the Joint Research Network on Advanced Materials and Systems (JONAS) program of BASF SE and ETH Zurich for scientific and financial support.

References

(1) Thompson, R. C.; Olsen, Y.; Mitchell, R. P.; Davis, A.; Rowland, S. J.; John, A. W. G.; McGonigle, D.; Russell, A. E. Lost at sea: where is all the plastic? *Science* **2004**, *304* (5672), 838.

(2) Rillig, M. C. Microplastic in Terrestrial Ecosystems and the Soil? *Environ Sci Technol* **2012**, *46* (12), 6453–6454.

(3) Browne, M. A.; Crump, P.; Niven, S. J.; Teuten, E.; Tonkin, A.; Galloway, T.; Thompson, R. Accumulation of Microplastic on Shorelines Woldwide: Sources and Sinks. *Environ Sci Technol* **2011**, *45* (21), 9175–9179.

(4) Puoci, F.; Iemma, F.; Spizzirri, U. G.; Cirillo, G.; Curcio, M.; Picci, N. Polymer in agriculture: a review. *American Journal of Agricultural and*

554 *Biological Sciences* **2008**, *3* (1), 299–314.
555 (5) Briassoulis, D.; Dejean, C.; Picuno, P. Critical Review of Norms and
556 Standards for Biodegradable Agricultural Plastics Part II: Composting. *J*
557 *Polym Environ* **2010**, *18* (3), 364–383.
558 (6) Stloukal, P.; Verney, V.; Commereuc, S.; Rychly, J.; Matisova-Rychlá, L.;
559 Pis, V.; Koutny, M. Assessment of the interrelation between photooxidation
560 and biodegradation of selected polyesters after artificial weathering.
561 *Chemosphere* **2012**, *88* (10), 1214–1219.
562 (7) Gross, R. A. Biodegradable Polymers for the Environment. *Science* **2002**, *297*
563 (5582), 803–807.
564 (8) Künkel, A.; Becker, J.; Börger, L.; Hamprecht, J.; Koltzenburg, S.; Loos, R.;
565 Schick, M. B.; Schlegel, K.; Sinkel, C.; Skupin, G.; Monotori, Y. *Ullmann's*
566 *Encyclopedia of Industrial Chemistry*; Wiley-VCH Verlag GmbH & Co.
567 KGaA: Weinheim, 2016; pp 1–29.
568 (9) Mueller, R.-J. Biological degradation of synthetic polyesters—Enzymes as
569 potential catalysts for polyester recycling. *Process Biochemistry* **2006**, *41*
570 (10), 2124–2128.
571 (10) Yamamoto-Tamura, K.; Hiradate, S.; Watanabe, T.; Koitabashi, M.;
572 Sameshima-Yamashita, Y.; Yarimizu, T.; Kitamoto, H. Contribution of soil
573 esterase to biodegradation of aliphatic polyester agricultural mulch film in
574 cultivated soils. *AMB Express* **2015**, *5* (1), 10.
575 (11) Tokiwa, Y.; Suzuki, T. Hydrolysis of polyesters by lipases. *Nature* **1977**, *270*
576 (5632), 76–78.
577 (12) Teeraphatpornchai, T.; Nakajima-Kambe, T.; Shigeno-Akutsu, Y.;
578 Nakayama, M.; Nomura, N.; Nakahara, T.; Uchiyama, H. Isolation and
579 characterization of a bacterium that degrades various polyester-based
580 biodegradable plastics. *Biotechnol. Lett.* **2003**, *25* (1), 23–28.
581 (13) Akutsu-Shigeno, Y.; Teeraphatpornchai, T.; Teamtisong, K.; Nomura, N.;
582 Uchiyama, H.; Nakahara, T.; Nakajima-Kambe, T. Cloning and sequencing
583 of a poly(DL-lactic acid) depolymerase gene from Paenibacillus amylolyticus
584 strain TB-13 and its functional expression in Escherichia coli. *Appl Environ*
585 *Microbiol* **2003**, *69* (5), 2498–2504.
586 (14) Rizzarelli, P.; Impallomeni, G.; Montaudo, G. Evidence for Selective
587 Hydrolysis of Aliphatic Copolyesters Induced by Lipase Catalysis.
588 *Biomacromolecules* **2004**, *5* (2), 433–444.
589 (15) Herrero Acero, E.; Ribitsch, D.; Steinkellner, G.; Gruber, K.; Greimel, K.;
590 Eiteljoerg, I.; Trotscha, E.; Wei, R.; Zimmermann, W.; Zinn, M.; Cavaco-
591 Paulo, A.; Freddi, G.; Schwab, H.; Guebitz, G. M. Enzymatic Surface
592 Hydrolysis of PET: Effect of Structural Diversity on Kinetic Properties of
593 Cutinases from Thermobifida. *Macromolecules* **2011**, *44* (12), 4632–4640.
594 (16) Ribitsch, D.; Yebra, A. O.; Zitzenbacher, S.; Wu, J.; Nowitsch, S.;
595 Steinkellner, G.; Greimel, K.; Doliska, A.; Oberdorfer, G.; Gruber, C. C.;
596 Schwab, H.; Stana-Kleinshek, K.; Herrero Acero, E.; Guebitz, G.M. Fusion
597 of Binding Domains to Thermobifida cellulosilytica Cutinase to Tune
598 Sorption Characteristics and Enhancing PET Hydrolysis. *Biomacromolecules*
599 **2013**, *14* (6), 1769–1776.
600 (17) Hajighasemi, M.; Nocek, B. P.; Tchigvintsev, A.; Brown, G.; Flick, R.; Xu,
601 X.; Cui, H.; Hai, T.; Joachimiak, A.; Golyshin, P. N.; Savchenko, A.;
602 Edwards, E. A.; Yakunin, A. F. Biochemical and Structural Insights into
603 Enzymatic Depolymerization of Polylactic Acid and Other Polyesters by

Microbial Carboxylesterases. *Biomacromolecules* **2016**, *17* (6), 2027–2039.
(18) Kleeberg, I.; Welzel, K.; VandenHeuvel, J.; Müller, R. J.; Deckwer, W. D. Characterization of a New Extracellular Hydrolase from Thermobifida fusca Degrading Aliphatic−Aromatic Copolyesters. *Biomacromolecules* **2005**, *6* (1), 262–270.
(19) Müller, R.-J.; Schrader, H.; Profe, J.; Dresler, K.; Deckwer, W.-D. Enzymatic Degradation of Poly(ethylene terephthalate): Rapid Hydrolyse using a Hydrolase fromT. fusca. *Macromolecular Rapid Communications* **2005**, *26* (17), 1400–1405.
(20) Yoshida, S.; Hiraga, K.; Takehana, T.; Taniguchi, I.; Yamaji, H.; Maeda, Y.; Toyohara, K.; Miyamoto, K.; Kimura, Y.; Oda, K. A bacterium that degrades and assimilates poly(ethylene terephthalate). *Science* **2016**, *351* (6278), 1196–1199.
(21) Ribitsch, D.; Heumann, S.; Trotscha, E.; Herrero Acero, E.; Greimel, K.; Leber, R.; Birner-Gruenberger, R.; Deller, S.; Eiteljoerg, I.; Remler, P.; Weber, T.; Siegert, P.; Maurer, K.-H., Donelli, I.; Freddi, G.; Schwab, H.; Guebitz, G. M. Hydrolysis of polyethyleneterephthalate by p-nitrobenzylesterase from Bacillus subtilis. *Biotechnol. Prog.* **2011**, *27* (4), 951–960.
(22) Marten, E.; Müller, R.-J.; Deckwer, W.-D. Studies on the enzymatic hydrolysis of polyesters I. Low molecular mass model esters and aliphatic polyesters. *Polymer Degradation and Stability* **2003**, *80* (3), 485–501.
(23) Herzog, K.; Müller, R. J.; Deckwer, W. D. Mechanism and kinetics of the enzymatic hydrolysis of polyester nanoparticles by lipases. *Polymer Degradation and Stability* **2006**, *91* (10), 2486–2498.
(24) Zumstein, M. T.; Kohler, H.-P. E.; McNeill, K.; Sander, M. Enzymatic Hydrolysis of Polyester Thin Films: Real-Time Analysis of Film Mass Changes and Dissipation Dynamics. *Environ Sci Technol* **2016**, *50* (1), 197–206.
(25) Perz, V.; Zumstein, M. T.; Sander, M.; Zitzenbacher, S.; Ribitsch, D.; Guebitz, G. M. Biomimetic Approach to Enhance Enzymatic Hydrolysis of the Synthetic Polyester Poly(1,4-butylene adipate): Fusing Binding Modules to Esterases. *Biomacromolecules* **2015**, *16* (12), 3889–3896.
(26) Grimm, J. B.; Heckman, L. M.; Lavis, L. D. *The Chemistry of Small-Molecule Fluorogenic Probes*, 1st ed.; Elsevier Inc., 2013; Vol. 113, pp 1–34.
(27) Leroy, E.; Bensel, N.; Reymond, J.-L. A low background high-Throughput screening (HTS) fluorescence assay for lipases and esterases using acyloxymethylethers of umbelliferone. *Bioorganic & Medicinal Chemistry Letters* **2003**, *13* (13), 2105–2108.
(28) Hosokawa, M.; Hoshino, Y.; Nishikawa, Y.; Hirose, T.; Yoon, D. H.; Mori, T.; Sekiguchi, T.; Shoji, S.; Takeyama, H. Biosensors and Bioelectronics. *Biosensors and Bioelectronic* **2014**, *67*, 1–7.
(29) Wallenstein, M. D.; Weintraub, M. N. Emerging tools for measuring and modeling the in situ activity of soil extracellular enzymes. *Soil Biology and Biochemistry* **2008**, *40* (9), 2098–2106.
(30) Shinozaki, Y.; Watanabe, T.; Nakajima-Kambe, T.; Kitamoto, H. K. Rapid and simple colorimetric assay for detecting the enzymatic degradation of biodegradable plastic films. *Journal of Bioscience and Bioengineering* **2013**, *115* (1), 111–114.
(31) Cornils, B.; Lappe, P. *Ullmann's Encyclopedia of Industrial Chemistry*;

654 Wiley-VCH Verlag GmbH & Co. KGaA: Weinheim, 2000; pp 1–19.
655 (32) Longhi, S.; Czjzek, M.; Lamzin, V.; Nicolas, A.; Cambillau, C. Atomic
656 resolution (1.0 A) crystal structure of Fusarium solani cutinase:
657 stereochemical analysis. *Journal of Molecular Biology* **1997**, *268* (4), 779–
658 799.
659 (33) Gasteiger, E.; Hoogland, C.; Gattiker, A.; Duvaud, S.; Wilkins, M.; Appel,
660 R.; Bairoch, A. *Protein identification and analysis tools on the ExPASy*
661 *server*; Humana Press: Totowa, NJ, 2005; pp 571–607.
662 (34) Baker, P. J.; Poultney, C.; Liu, Z.; Gross, R.; Montclare, J. K. Identification
663 and comparison of cutinases for synthetic polyester degradation. *Appl*
664 *Microbiol Biotechnol* **2011**, *93* (1), 229–240.
665 (35) Derewenda, U.; Swenson, L.; Wei, Y. Y.; Green, R.; Kobos, P. M.; Joerger,
666 R.; Haas, M. J.; Derewenda, Z. S. Conformational Lability of Lipases
667 Observed in the Absence of an Oil-Water Interface - Crystallographic Studies
668 of Enzymes From the Fungi Humicola-Lanuginosa and Rhizopus-Delemar. *J.*
669 *Lipid Res.* **1994**, *35* (3), 524–534.
670 (36) Ribitsch, D.; Herrero Acero, E.; Greimel, K.; Dellacher, A.; Zitzenbacher, S.;
671 Marold, A.; Rodriguez, R. D.; Steinkellner, G.; Gruber, K.; Schwab, H.;
672 Guebitz, G. A New Esterase from Thermobifida halotolerans Hydrolyses
673 Polyethylene Terephthalate (PET) and Polylactic Acid (PLA). *Polymers*
674 **2012**, *4* (4), 617–629.
675 (37) Goddard, J.-P.; Reymond, J.-L. Recent advances in enzyme assays. *Trends in*
676 *Biotechnology* **2004**, *22* (7), 363–370.
677 (38) Mangel, W. F.; Livingston, D. C.; Brocklehurst, J. R.; Cannon, J. F.; Leytus,
678 S. P.; Peltz, S. W.; Pelta, G. A.; Liu, H. Y. A new active-site titrant of serine
679 proteases. *Meth. Enzymol.* **1981**, *80 Pt C*, 414–424.
680 (39) Chen, S.; Su, L.; Chen, J.; Wu, J. Biotechnology Advances. *Biotechnology*
681 *Advances* **2013**, *31* (8), 1754–1767.
682 (40) Witt, U.; Müller, R. J.; Deckwer, W. D. Biodegradation of Polyester
683 Copolymers Containing Aromatic Compounds. *Journal of Macromolecular*
684 *Science, Part A* **1995**, *32* (4), 851–856.
685 (41) Tokiwa, Y.; Suzuki, T.; Takeda, K. Two Types of Lipases in Hydrolysis of
686 Polyester. *Agricultural and Biological Chemistry* **1988**, *52* (8), 1937–1943.
687 (42) Khan, M. A.; Idriss Ali, K. M.; Yoshii, F.; Makuuchi, K. Enzymatic
688 degradation of Bionolle and Bionolle–rubber blends. *Polymer Degradation*
689 *and Stability* **1999**, *63* (2), 261–264.
690 (43) Eberl, A.; Heumann, S.; Brückner, T.; Araujo, R.; Cavaco-Paulo, A.;
691 Kaufmann, F.; Kroutil, W.; Guebitz, G. M. Enzymatic surface hydrolysis of
692 poly(ethylene terephthalate) and bis(benzoyloxyethyl) terephthalate by lipase
693 and cutinase in the presence of surface active molecules. *J. Biotechnol.* **2009**,
694 *143* (3), 207–212.
695 (44) Jaeger, K.-E.; Ransac, S.; Dijkstra, B. W.; Colson, C.; van Heuvel, M.;
696 Misset, O. Bacterial lipases. *FEMS Microbiol. Rev.* **1994**, *15* (1), 29–63.
697 (45) Dutta, K.; Sen, S.; Veeranki, V. D. Production, characterization and
698 applications of microbial cutinases. *Process Biochemistry* **2009**, *44* (2), 127–
699 134.
700 (46) Ronkvist, Å. M.; Xie, W.; Lu, W.; Gross, R. A. Cutinase-Catalyzed
701 Hydrolysis of Poly(ethylene terephthalate). *Macromolecules* **2009**, *42* (14),
702 5128–5138.
703 (47) Araujo, R.; Silva, C.; O'Neill, A.; Micaelo, N.; Guebitz, G.; Soares, C. M.;

Casal, M.; Cavaco-Paulo, A. Tailoring cutinase activity towards polyethylene terephthalate and polyamide 6,6 fibers. *J. Biotechnol.* **2007**, *128* (4), 849–857.

(48) Silva, C.; Da, S.; Silva, N.; Matamá, T.; Araujo, R.; Martins, M.; Chen, S.; Chen, J.; Wu, J.; Casal, M.; Cavaco-Paulo, A. Engineered Thermobifida fusca cutinase with increased activity on polyester substrates. *Biotechnology Journal* **2011**, *6* (10), 1230–1239.

(49) Bornscheuer, U. T. Feeding on plastic. *Science* **2016**, *351* (6278), 1154–1155.

(50) Kobayashi, S.; Uyama, H.; Takamoto, T. Lipase-Catalyzed Degradation of Polyesters in Organic Solvents. A New Methodology of Polymer Recycling Using Enzyme as Catalyst. *Biomacromolecules* **2000**, *1* (1), 3–5.

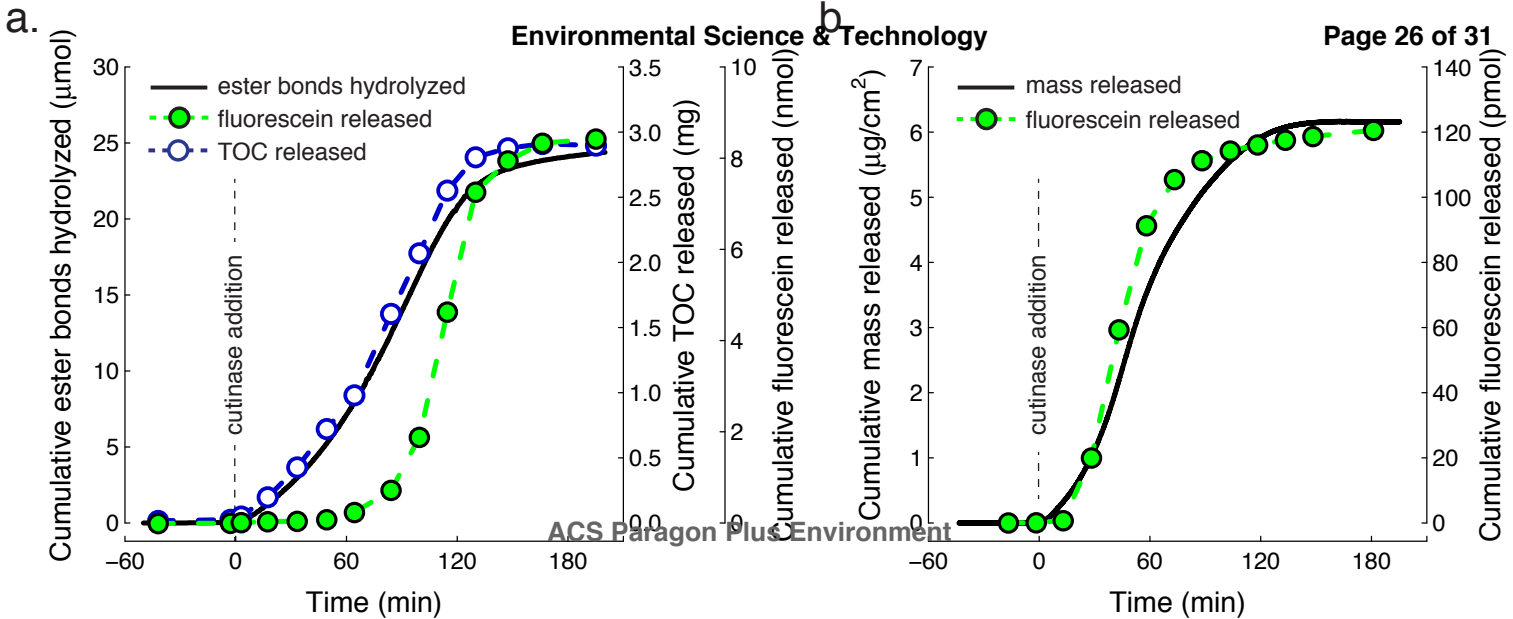

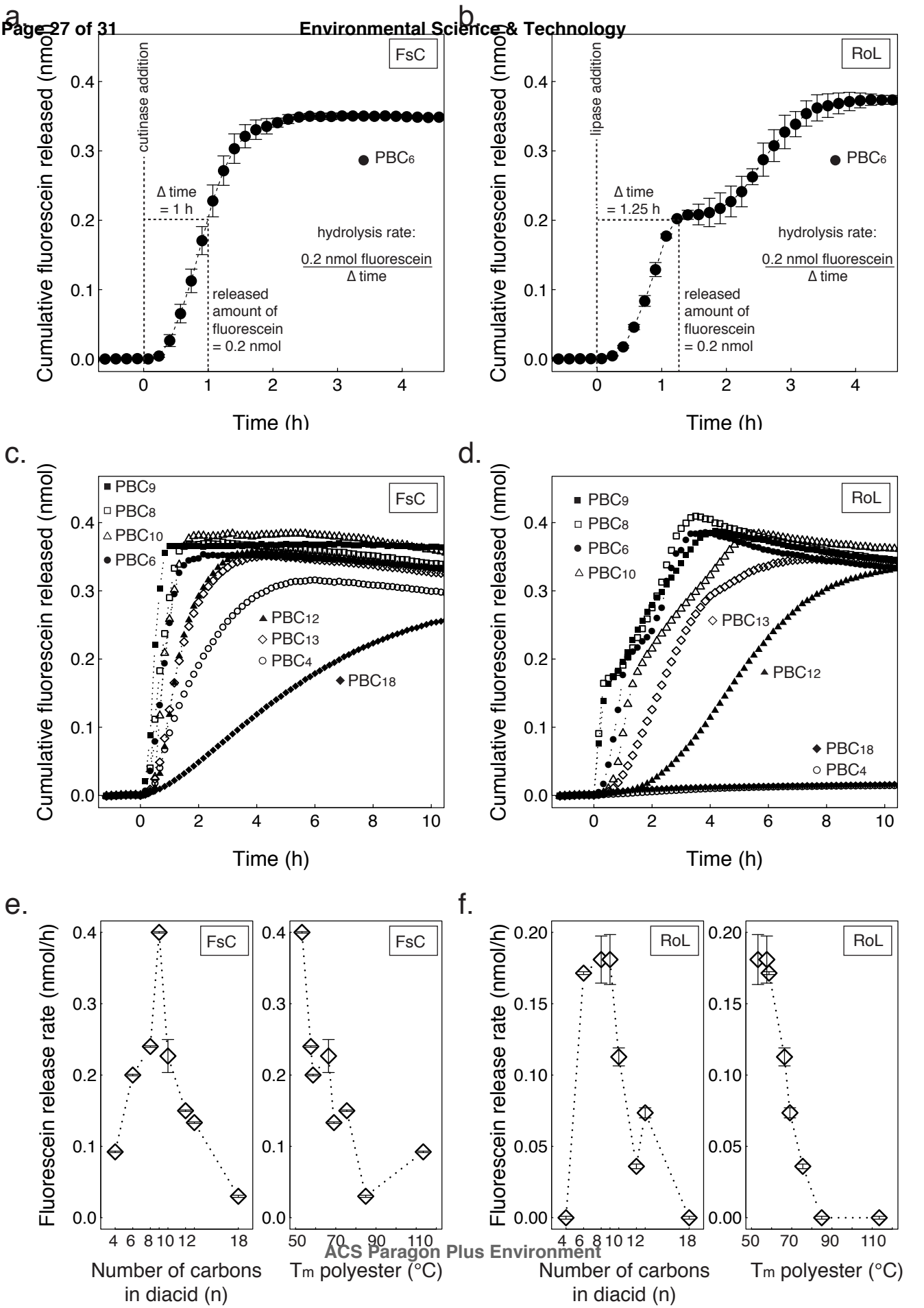

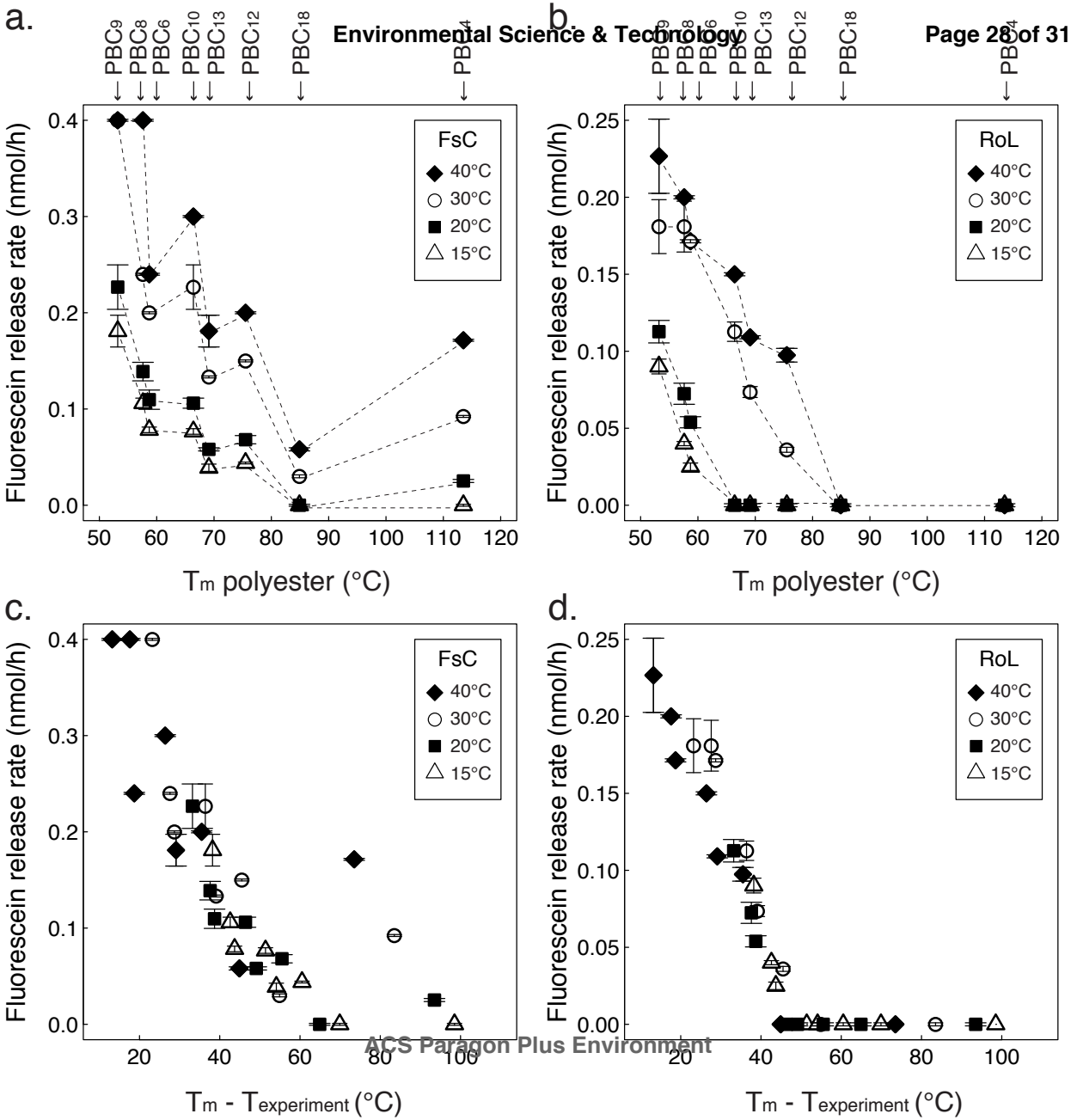

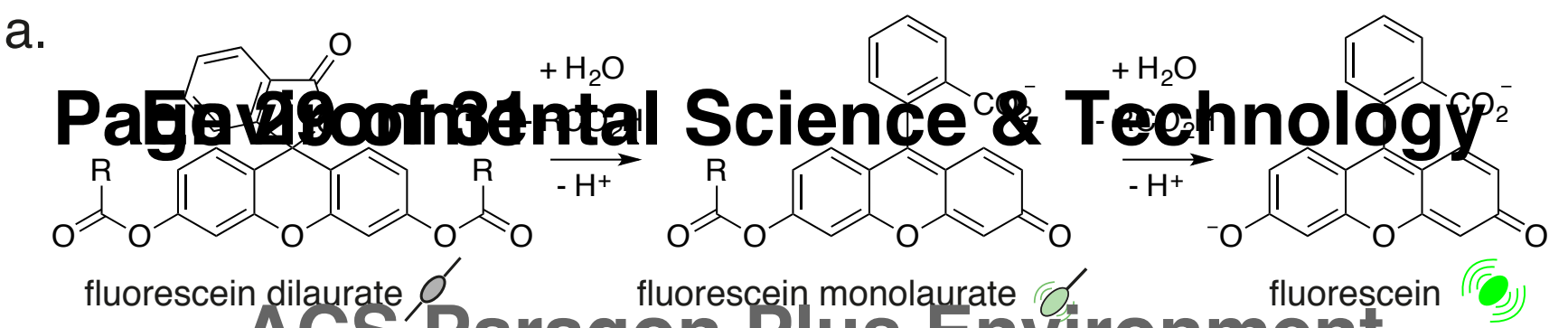

Generalized structure PBC_n:

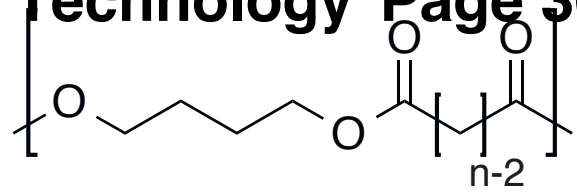

Abbreviation	Number of carbon atoms in diacid (n)	T_m (°C)	M_n (g/mol)	M_w (g/mol)
PBC_4	4	113.5	22700	112000
PBC_6	6	58.7	19800	52100
PBC_8	8	57.6	28100	94700
PBC_9	9	53.2	25700	102000
PBC_{10}	10	66.4	23700	95400
PBC_{12}	12	75.5	28300	91300
PBC_{13}	13	69.1	25700	78000
PBC_{18}	18	84.9	n.m	n.m